

Direct formation of new water soluble Re and Tc complexes containing PTA (1,3,5-triaza-7-phosphaadamantane) from their permethylated salts. Reactivity and X-ray crystal structures.

Lorenza Marvelli,^{*a} Paola Bergamini,^a Andrea Marchi,^a Giada Bersani,^a Valeria Ferretti,^b Valerio Bertolasi.^b

^a Dipartimento di Scienze Chimiche e Farmaceutiche, Università degli Studi di Ferrara, Via Luigi Borsari, 46, 44121 Ferrara, Italy.

^b Centro di Strutturistica Diffraattometrica, Dipartimento di Scienze Chimiche e Farmaceutiche, Università degli Studi di Ferrara, Via Luigi Borsari, 46, 44121 Ferrara, Italy.

Keywords: Water-soluble complexes / Rhenium / Technetium / 1,3,5-Triaza-7-phosphaadamantane / Dithiocarbamate complexes/ X-ray structures

* *In honour of Carlo Mealli on the occasion of his 70th birthday.*

Abstract

A new *one-pot* synthetic procedure to new water-soluble rhenium and technetium complexes, directly from the corresponding permethylated species, is here presented. The new water-soluble M(IV) and M(III), (M = Re, Tc) paramagnetic complexes were obtained by treating $[\text{MO}_4]^-$ with an excess of PTA (1,3,5-triaza-7-phosphaadamantane), in water. In the presence of SnCl_2 , the complexes $[\text{MCl}_3(\text{PTA})_3]\text{Cl}$, (M = Re, **1**; Tc, **3**), were obtained in good yield, while in the absence of SnCl_2 the unexpected species containing methylated PTA, $[\text{MCl}_4(\text{PTA-Me})_2]\text{Cl}$, (M = Re, **2**; Tc, **4**), were produced. A preliminary study of the reactivity of these products with *N,N*-diethyldithiocarbamate was also carried out: the diamagnetic binuclear μ -oxo species $[\text{M}_2\text{O}_3(\text{Et}_2\text{NCS}_2)_4]$ (M = Re, **6**; Tc, **7**) were isolated from the reactions of **1**, **2** and **4** with dithiocarbamate. The reaction of **3** gave rise to an unusual *epta*-coordinated technetium(III) complex $[\text{Tc}(\text{Et}_2\text{NCS}_2)_3(\text{PTA})]$ (**5**). The X-ray crystal structures of the new PTA complexes **2**, **4**, **5** and **7** have been determined.

1. Introduction

Rhenium and Technetium complexes continue to attract scientific interest for therapeutic and diagnostic applications. In this regard, the development of *one-pot* synthetic procedures for obtaining new complexes or intermediates under mild conditions is a relevant issue for applications in nuclear medicine as imaging agents ($^{99\text{m}}\text{Tc}$) or therapeutic purposes (^{186}Re , ^{188}Re) [1-7]. The rich coordination chemistry of Tc and Re, owing to their variety of oxidation states ranging from -1 to $+7$, allowed to obtain several versatile precursors such as *oxo*-Tc/Re(V)

$[M=O]^{3+}$, *nitrido*-Tc/Re(V) $[M\equiv N]^{2+}$, *hydrazido*-Tc/Re (III) $[MNNR]^{n+}$ and *carbonyl*-Tc/Re(I) *fac*- $[M(CO)_3]^+$, which have been exploited for developing new radiopharmaceuticals [8-11].

While non-radioactive metal based anticancer drugs can be synthesized in a wide choice of media including organic solvents, for ^{99m}Tc or ^{188}Re radiodrugs the preparation in water is mandatory. In fact, this invariably starts from $^{99}\text{Mo}/^{99m}\text{Tc}$ and $^{188}\text{W}/^{188}\text{Re}$ respectively [12], eluted from their generators in aqueous solutions and then treated with the appropriate ligands. Water soluble products are formed *in situ* and their aqueous solutions are directly employed as pharmaceutical forms for intravenous administration.

Transition-metal complexes can be made water-soluble through the coordination of hydrophilic ligands and, for this purpose, the phosphine PTA (1,3,5-triaza-7-phosphaadamantane) has attracted particular attention in medicine applications due to its high water-solubility, easy synthesis, resistance to oxidation and air-stability [13,14]. Another important feature of PTA is that all the positions of the cage structure are reactive in specific conditions, allowing to design and to prepare families of PTA derivatives (e.g. *N*-alkylation, methylene functionalization) presenting some of the parent compound properties [13, 15-18]. In our previous work, we reported the synthesis and characterization of new water-soluble Re(V) *oxo*- and *nitrido*-complexes, $[\text{ReO}_2\text{Cl}(\text{PTA})_3]$, $[\text{ReNCl}_2(\text{PTA})_3]$, obtained by ligand substitution with PTA [19] in $[\text{ReNCl}_2(\text{L})_2]$ and $[\text{ReOCl}_2\text{X}(\text{L})_2]$ ($\text{X}^- = \text{Cl}, \text{OMe}, \text{OEt}$; $\text{L} = \text{PPh}_3$) that are commonly used as starting precursors.

In this paper we describe a new *one-pot* synthetic procedure which produces new water soluble M(IV) and M(III) complexes in good yields, starting from the permetallated species $[\text{MO}_4]^-$, ($\text{M} = \text{Re}, \text{Tc}$). A preliminary study of the reactivity of these products with *N,N*-diethyldithiocarbamate is also described herein.

2. Experimental

2.1. Materials and instruments

All the manipulations were carried out in air atmosphere. Commercial solvents and reagents were purchased and used without further purification. PTA (1,3,5-triaza-7-phosphaadamantane) and (PTA-Me)I were prepared according to literature procedures [20, 21]. Elemental analyses were determined using a CHNS-O Analyzer, FLASH 2000 - Organic Elemental Analyzer Thermo Scientific. Mass spectra were acquired with an Electrospray MS ($\text{CH}_3\text{CN}/\text{MeOH}$) Micromass LCQ Duo Finnigan. FT-IR spectra were recorded on a Bruker Vertex 70 FT-IR instrument

(4000–400 cm^{-1} , KBr), using a Spectra-Tech collector diffuse reflectance accessory. NMR spectra were recorded on a Varian Gemini 300 MHz spectrometer (^1H at 300.13 MHz, ^{31}P at 121.50 MHz). ^{31}P NMR spectra were run with proton decoupling and signals are reported in ppm relative to an external 85% H_3PO_4 standard.

Caution! ^{99}Tc is a weak β -emitter ($E_\beta = 0.292$ MeV, $t_{1/2} = 2.12 \cdot 10^5$ years). All manipulations were carried out in a laboratory approved for low-level radioactivity.

2.2. Synthesis of $[\text{ReCl}_3(\text{PTA})_3]\text{Cl}$, **1**

A large excess of HCl (1 mL, 12M) was added to a solution of KReO_4 (50 mg, 0.17 mmol) in 10 mL of water. The mixture was stirred and gently heated at 40°C ; solid SnCl_2 (64 mg, 0.34 mmol) was added in small portions and the mixture changed its color from colorless to deep green. PTA (214 mg, 1.36 mmol) was slowly added until a clear persistent orange solution is achieved. Slow evaporation of the solvent at room temperature gave dark orange microcrystals, which were collected and washed with MeOH and Et_2O ; 85% yield, based on KReO_4 . ^1H NMR (300.13 MHz, D_2O , 25°C) δ (ppm): 6.78 (d, 6H, $\text{NCH}_2\text{N}_{\text{mer}}$, $^2J_{\text{HH}} = 12.9$ Hz), 7.44 (d, 12H, $\text{NCH}_2\text{N}_{\text{fac+mer}}$, $^2J_{\text{HH}} = 12.9$ Hz), 10.53 (d, 6H, $\text{NCH}_2\text{N}_{\text{mer}}$, $^2J_{\text{HH}} = 12.9$ Hz), 10.91 (d, 12H, $\text{NCH}_2\text{N}_{\text{fac+mer}}$, $^2J_{\text{HH}} = 12.9$ Hz), 11.62 (s, 12H, $\text{PCH}_2\text{N}_{\text{mer}}$), 13.20 (s, 24H, $\text{PCH}_2\text{N}_{\text{fac+mer}}$). MS-ESI: observed m/z 764 ($I = 80\%$), calculated 764,03 for $[\text{C}_{18}\text{H}_{36}\text{Cl}_3\text{N}_9\text{P}_3\text{Re}]^+$. FT-IR (KBr, cm^{-1}): 3521 (br s, H_2O), 2983 (br m, CH), 1666 (m, H_2O), 1451 (m), 1417 (m), 1283 (m), 1242 (s), 1015 (s), 981 (s), 950 (m), 813 (m), 577(m), PTA. $S_{20^\circ\text{C}}$ (H_2O): 0.8 g mL^{-1} .

2.3. Synthesis of $[\text{ReCl}_4(\text{PTA-Me})_2]\text{Cl}$, **2**

Method A. A large excess of HCl conc. (1 mL, 12M) was added to a solution of KReO_4 (50 mg, 0.17 mmol) in 10 mL of water; the mixture was kept under stirring and mild heating (40°C) then an excess of solid PTA (214 mg, 1.36 mmol) was slowly added. The colour of the mixture rapidly changes from yellow to orange and, finally, a clear brown solution was obtained. After *ca.* 40 minutes the solution was concentrated at room temperature and brown-orange crystals were collected, washed with MeOH and Et_2O ; 51 % yield, based on KReO_4 .

Method B. Complex **2** may also be prepared, in about 15 minutes, under conditions similar to those above described, but adding (PTA-Me)I (204 mg, 0.68 mmol) instead of PTA. Slow evaporation of the solvent at room temperature, afforded brown crystals of **2**, in greater yield than in method A, (86 %).

Method C. Reacting KReO_4 (50 mg, 0.17 mmol) in acid water solution (10 mL of H_2O , 1 mL of HCl conc.), with PTA (214 mg, 1.36 mmol) and adding 1 mL of formaldehyde (37% wt in water

solution), complex **2** was obtained in 30 minutes and in good yield, (81%). ^1H NMR (300.13 MHz, D_2O , 25°C) δ (ppm): (A, 80%) 5.19 (s, 6H, CH_3), 5.56 (br d, 2H, NCH_2N , $^2J_{\text{HH}}=13.5$ Hz), 7.50 (br d, 4H, NCH_2N^+ , $^2J_{\text{HH}}=13.9$ Hz), 7.61 (d, 4H, PCH_2N , $^2J_{\text{HP}}=12.0$ Hz), 10.11 (br d, 2H, NCH_2N , $^2J_{\text{HH}}=13.5$ Hz), 10.55 (br s, 4H, PCH_2N^+), 10.64 (d, 4H, PCH_2N , $^2J_{\text{HP}}=12.0$ Hz), 11.77 (br d, 4H, NCH_2N^+ , $^2J_{\text{HH}}=13.9$ Hz).

(B, 20%): 5.04 (s, 6H, CH_3), 5.55 (br d, 2H, CH_2), 7.39 (br d, 2H, CH_2), 7.82 (br d, 4H, CH_2), 9.51 (m, 6H, CH_2), 10.30 (m, 6H, CH_2), 10.79 (br d, 2H, CH_2), 11.44 (br d, 2H, CH_2) ppm. MS-ESI: observed m/z 672 ($I=54\%$), calcd. 672.39 for $\text{C}_{14}\text{H}_{30}\text{Cl}_4\text{N}_6\text{P}_2\text{Re}$ (M^+). Anal. Calc. for $\text{C}_{14}\text{H}_{30}\text{Cl}_5\text{N}_6\text{P}_2\text{Re}$ (707.84): C, 23.75; H, 4.27; N, 11.87 %. Found: C, 23.68; H, 4.25; N, 11.79 %. FT-IR (KBr, cm^{-1}): 3450 (br s, H_2O), 2980 (br m, CH), 1665 (m, H_2O), 1456 (m), 1411 (m), 1282 (m), 1245 (s), 1018 (s), 984 (s), 953 (m), 801 (m), 570 (m), PTA. $S_{20}^\circ\text{C}$ (H_2O): 0.6 g mL^{-1} .

2.4. NMR investigation of the formation of complex 2. A 5-mm screw-cap NMR tube was charged with a solution of KReO_4 (10 mg, $3.4 \cdot 10^{-2}$ mmol) and PTA (43 mg, 0.27 mmol) in D_2O (0.8 ml); an excess of HCl (200 μL) was added and the reaction was monitored by NMR spectroscopy. The formation of $[\text{PTA}(\text{H})]^+$ was immediate and confirmed by ^{31}P NMR (-90.88 ppm). When the yellow solution was heated at 40°C in oil bath, after 10 minutes, small bubbles of formaldehyde were formed, as confirmed by a singlet at 9.9 ppm in the protonic spectrum. Heating was continued for another 20 minutes and its colour slowly changed from yellow to deep red. In the corresponding ^{31}P NMR, signals at -3.14 ppm, -85.50 ppm and -90.88 ppm confirmed the presence of $[\text{PTA}(\text{O})]$, $[\text{PTA}(\text{Me})]^+$ and $[\text{PTA}(\text{H})]^+$ respectively, while the formation of the paramagnetic complex **2** was observable by ^1H NMR.

2.5. Reduction of pertechnetate with SnCl_2 , **3**

To an aqueous solution of NH_4TcO_4 (40 mg, 0.22 mmol in 10 mL of H_2O) under mild heating (30°C) and stirring, 1 mL of HCl (12M), 2 equivalents of SnCl_2 (84 mg) and PTA (209 mg, 1.33 mmol) were added in sequence. A red solid was rapidly obtained and the reaction mixture was stirred for other 20 minutes. Complex **3** was separated as a solid, was filtered, washed with water and dried with MeOH and Et_2O . Complex **3** is tentatively formulated as $[\text{TcCl}_3(\text{PTA})_3]\text{Cl}$. ^1H NMR (300.13 MHz, DMSO-d_6 , 25°C) δ (ppm): 8.2 – 10.0 (br m, CH_2 , PTA).

2.6. Synthesis of $[\text{TcCl}_4(\text{PTA-Me})_2]\text{Cl}$, **4**

An aqueous solution of NH_4TcO_4 (40 mg, 0.22 mmol in 10 mL of H_2O) was treated with 3 drops of HCl (12M) at 30°C . An excess of solid PTA (209 mg, 1,33 mmol) was added under stirring in

small portions. The mixture became turbid and dark then, after few minutes, turned to a clear orange-red solution. The reaction was completed in about 25 minutes. Slow evaporation of the solvent at room temperature, gave red crystals, separated and washed with MeOH and Et₂O; 79 % yield, based on NH₄TcO₄. ¹H NMR (300.13 MHz, DMSO-d₆, 25°C) δ (ppm): 3.0 (br s, 6H, CH₃), 7.4 (br m, 4H, CH₂, PTA), 8.0 (br m, 4H, CH₂, PTA), 9.9 (br m, 8H, CH₂, PTA), 13.4 (br m, 8H, CH₂, PTA) ppm. S_{20 °C} (H₂O): 0.56 g mL⁻¹.

2.7. Synthesis of complex [Tc(Et₂NCS₂)₃(PTA)], **5**

Complex **3** (50 mg), was dissolved in methanol/acetone (1:1, 6 mL) and treated with a solution containing an excess of Na(Et₂NCS₂) (95 mg, 0.41 mmol), solubilized in a minimum quantity of acetone. The resulting solution was gently heated for 15 minutes. Yellow-brown microcrystals of **5** were obtained after evaporation of the solvents at room temperature, washed with MeOH and Et₂O; yield 79 %. ¹H NMR (300.13 MHz, CDCl₃, 25°C) δ (ppm): 1.3 (br t, 18H, CH₃), 4.0 (m, 12H, CH₂, PTA), 4.4 (m, 12H, CH₂).

2.8. Reaction of **1** and **2** with Na(Et₂NCS₂)

Na(Et₂NCS₂) (30 mg, 0.13 mmol) dissolved in the minimum volume of acetone, was added to an aqueous solution of **1** (50 mg, 0.06 mmol). The reaction mixture was kept at room temperature for 30 minutes under stirring. A dark-yellow precipitate was separated from the mother liquor, collected and washed with water, MeOH and Et₂O. The solid was then re-dissolved in CH₂Cl₂ and EtOH was added; slow evaporation of the solvents at room temperature left brown-yellow crystals of the known *μ*-oxo complex [Re₂O₃(Et₂NCS₂)₄], **6** [22]. Analytical and spectroscopic data were coincident with those reported in the literature, (85 % yield). Replacing **1** with complex **2** in the above described procedure, pure complex **6** was obtained.

2.9. Synthesis of complex *μ*-oxo [Tc₂O₃(Et₂NCS₂)₄], **7**

Na(Et₂NCS₂) (56 mg, 0.25 mmol) dissolved in the minimum volume of acetone (1 mL) was added to a solution of **4** (70 mg, 0.10 mmol) in water (5 mL). The reaction mixture was kept at room temperature for 30 minutes under stirring. A dark-yellow precipitate was collected, washed with water, MeOH and Et₂O and recrystallized by CH₂Cl₂ / EtOH (1:1); yield 80 %. ¹H NMR (300.13 MHz, CD₂Cl₂, 25°C) δ (ppm): 1.2 – 1.5 (m, 24H, CH₃), 3.8 – 4.0 (m, 16H, CH₂).

2.10. X-ray crystallography

The crystallographic data for the title compounds were collected on a Nonius Kappa CCD diffractometer at room temperature using graphite-monochromated MoK α radiation ($\lambda = 0.71073$ Å). Data sets were integrated with the Denzo-SMN package [23] and corrected for Lorentz-polarization and absorption effects [24]. The experimental details of the data collections are summarized in Table 1. The structure was solved by direct methods (SIR97) [25] and refined by full-matrix least-squares methods with all non-hydrogen atoms anisotropic. In complex **7** the terminal ethyl groups of the (Et₂NCS₂)⁻ ligands were found to be disordered; however, any attempt to model such a disorder did not made significant improvements to the structure quality. All C-H hydrogen atoms were included on calculated positions, riding on their carrier atoms. In **4**, the hydrogens belonging to the co-crystallized water molecules have not been located in the Difference Fourier map and were not included in the refinement. All calculations were performed using SHELXL-97 [26] implemented in the WINGX system of programs [27]. In **2**, the electron density difference map showed some rather large, broad peaks located among the complexes. Attempts to identify the solvent molecules failed. Instead, a new set of F^2 (hkl) values with the contribution from solvent molecules withdrawn was obtained by the *SQUEEZE* procedure implemented in *PLATON* [28]. The potential solvent volume in the crystals is 172 Å³ per unit cell volume. Experimental details are given in Table 1. Selected bond distances and angles are given in Table 2 while geometrical parameters for C-H...X interactions are reported in Table S1 (Supplementary Materials). We have considered only contacts where C-H...X angles are greater than 130° and H...X distances are shorter than the sum of the van der Waals radii.

Crystallographic data for the structure reported in this paper have been deposited with the Cambridge Crystallographic Data Centre as supplementary publication no. **CCDC 1535902-1535905**. Copies of the data can be obtained free of charge on application to CCDC, 12 Union Road, Cambridge CB2 1EZ, UK (Fax: ((44) 1223 336-033; e-mail: deposit@ccdc.cam.ac.uk).

Table 1. Experimental details

	2	4	5	7
Chemical formula	C ₁₄ H ₃₀ Cl ₄ N ₆ P ₂ Re·Cl · <i>n</i> H ₂ O	C ₁₄ H ₃₀ Cl ₄ P ₂ TcN ₆ ·Cl · 3(H ₂ O)	C ₂₁ H ₄₂ N ₆ PS ₆ Tc	C ₂₀ H ₄₀ N ₄ O ₃ S ₈ Tc ₂
M_r	707.83	674.54	700.85	838.86
Crystal system, space group	Triclinic, $P\bar{1}$	Monoclinic, $P2_1/n$	Triclinic, $P\bar{1}$	Monoclinic, $P2_1/n$
a, b, c (Å)	7.7986 (1) 12.6791 (2) 13.9645 (3)	11.0270 (2) 11.3150 (2) 20.6116 (4)	11.1510 (3) 11.2467 (3) 13.7193 (4)	15.3213 (5) 14.1384 (4) 16.3405 (6)
α, β, γ (°)	70.8498 (7) 86.7113 (7) 89.0660 (11)	90 92.4705 (7)	80.7887 (12) 79.0571 (14) 68.7911 (12)	90 93.9465 (13) 90
V (Å ³)	1302.24 (4)	2569.33 (8)	1566.99 (8)	3531.3 (2)
Z	2	4	2	4
μ (mm ⁻¹)	5.32	1.23	0.93	1.28
Crystal size (mm)	0.38 × 0.26 × 0.12	0.28 × 0.17 × 0.14	0.28 × 0.12 × 0.05	0.19 × 0.14 × 0.07

No. of measured, independent and observed [$I > 2\sigma(I)$] reflections	18555, 7526, 6503	16390, 371, 213	20521, 7423, 4929	20207, 8198, 5945
R_{int}	0.062	0.026	0.069	0.039
$R[F^2 > 2\sigma(F^2)], wR(F^2), S$	0.035, 0.090, 1.04	0.041, 0.101, 1.07	0.048, 0.111, 0.97	0.038, 0.092, 1.07
No. of reflections	7526	7371	7423	8198
No. of parameters	255	282	322	342
$\Delta\rho_{\text{max}}, \Delta\rho_{\text{min}}$ (e Å ⁻³)	1.11, -2.85	1.77, -0.68	0.61, -1.05	0.57, -0.78

Table 2. Selected bond distances and angles (Å, °) for complexes **2, 4, 5** and **7**.

Complex 2			
Re1 - CL1	2.4482(9)	Re1 - CL4	2.362(1)
Re1 - CL2	2.449(1)	Re1 - P1	2.3663(8)
Re1 - CL3	2.349(1)	Re1 - P2	2.364(1)
Cl1 - Re1 - Cl2	85.26(4)	Cl2 - Re1 - P1	89.54(4)
Cl1 - Re1 - Cl3	92.23(4)	Cl3 - Re1 - P1	87.68(3)
Cl1 - Re1 - Cl4	90.72(4)	Cl3 - Re1 - P2	86.30(4)
Cl1 - Re1 - P2	87.93(3)	Cl4 - Re1 - P1	89.72(3)
Cl2 - Re1 - Cl3	92.51(4)	Cl4 - Re1 - P2	89.99(4)
Cl2 - Re1 - Cl4	91.53(4)	P1 - Re1 - P2	97.25(3)
Complex 4			
Tc1 - CL1	2.4473(9)	Tc1 - CL4	2.3465(8)
Tc1 - CL2	2.4457(7)	Tc1 - P1	2.3650(7)
Tc1 - CL3	2.3534(8)	Tc1 - P2	2.3643(7)
Cl1 - Tc1 - Cl2	85.95(3)	Cl2 - Tc1 - P1	89.82(3)
Cl1 - Tc1 - Cl3	92.51(3)	Cl3 - Tc1 - P1	83.69(3)
Cl1 - Tc1 - Cl4	94.66(3)	Cl3 - Tc1 - P2	88.80(3)
Cl1 - Tc1 - P2	88.32(3)	Cl4 - Tc1 - P1	89.60(3)
Cl2 - Tc1 - Cl3	93.43(3)	Cl4 - Tc1 - P2	85.45(3)
Cl2 - Tc1 - Cl4	93.03(3)	P1 - Tc1 - P2	96.02(2)
Complex 5			
Tc1 - S1	2.4903(9)	Tc1 - S5	2.502(1)
Tc1 - S2	2.4728(9)	Tc1 - S6	2.4151(9)
Tc1 - S3	2.4786(8)	Tc1 - P1	2.294(1)
Tc1 - S4	2.487(1)		
S1 - Tc1 - S2	68.3(3)	S3 - Tc1 - S4	67.94(3)
S1 - Tc1 - S3	139.5(3)	S3 - Tc1 - S5	94.12(3)
S1 - Tc1 - S4	73.64(3)	S3 - Tc1 - S6	76.62(3)
S1 - Tc1 - S5	98.28(3)	S3 - Tc1 - P1	83.67(3)
S1 - Tc1 - S6	143.76(3)	S4 - Tc1 - S5	90.18(3)
S1 - Tc1 - P1	88.54(3)	S4 - Tc1 - S6	138.44(3)
S2 - Tc1 - S3	150.72(3)	S4 - Tc1 - P1	96.43(3)
S2 - Tc1 - S4	141.29(3)	S5 - Tc1 - S6	70.98(3)
S2 - Tc1 - S5	88.45(3)	S5 - Tc1 - P1	171.63(3)
S2 - Tc1 - S6	76.72(3)	S6 - Tc1 - P1	100.64(3)
S2 - Tc1 - P1	89.58(3)		
Complex 7			
Tc1 - S1	2.4867(9)	Tc2 - S5	2.4464(9)
Tc1 - S2	2.4301(9)	Tc2 - S6	2.455(1)
Tc1 - S3	2.406(1)	Tc2 - S7	2.4553(9)
Tc1 - S4	2.4637(8)	Tc2 - S8	2.4196(9)
Tc1 - O1	1.675(2)	Tc2 - O2	1.916(2)
Tc1 - O2	1.893(2)	Tc2 - O3	1.671(2)

S1 - Tc1 - S2	72.00(3)	S5 - Tc2 - S6	71.52(3)
S1 - Tc1 - S4	109.99(3)	S5 - Tc2 - S8	106.66(3)
S1 - Tc1 - O1	89.38(9)	S5 - Tc2 - O2	87.67(6)
S1 - Tc1 - O2	84.62(6)	S5 - Tc2 - O3	93.07(8)
S2 - Tc1 - S3	105.10(3)	S6 - Tc2 - S7	109.00(3)
S2 - Tc1 - O1	93.63(9)	S6 - Tc2 - O2	84.92(6)
S2 - Tc1 - O2	87.79(6)	S6 - Tc2 - O3	93.95(9)
S3 - Tc1 - S4	72.29(3)	S7 - Tc2 - S8	71.88(3)
S3 - Tc1 - O1	97.25(9)	S7 - Tc2 - O2	87.10(6)
S3 - Tc1 - O2	88.89(6)	S7 - Tc2 - O3	92.18(8)
S4 - Tc1 - O1	91.74(9)	S8 - Tc2 - O2	85.41(6)
S4 - Tc1 - O2	87.09(6)	S8 - Tc2 - O3	95.75(9)
O1 - Tc1 - O2	173.1(1)	O2 - Tc2 - O3	178.4(1)

3. Results and discussion

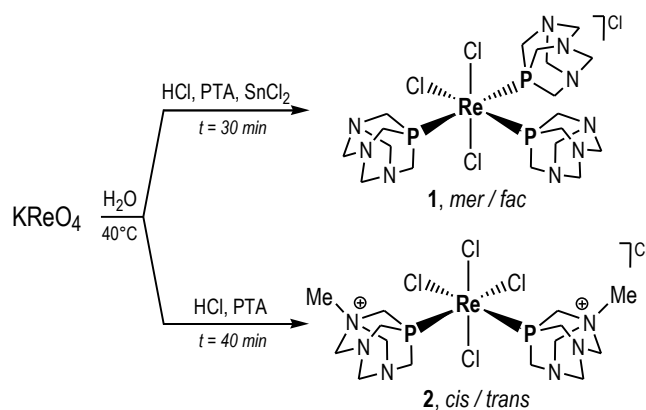
3.1. Rhenium complexes **1** and **2**

In the attempt to obtain *oxo*-rhenium complexes with the hydrosoluble phosphine PTA, we treated KReO_4 with two equivalents of SnCl_2 and an 8-fold molar amount of PTA in aqueous HCl (12M). The treatment of perrhenate salts with phosphines, acting both as reducing agents and as ligands, generally yields Re(V) *oxo*-complexes. A different behavior was expected for the water-soluble phosphine PTA which, due to its high resistance to oxidation, should act exclusively as a classic monodentate P donor ligand.

It is usual practice for the preparation of radiopharmaceuticals based on rhenium and technetium to add a tin salt to the reaction mixture in order to favor the reduction of rhenium and the formation of water soluble *oxo*-complexes. We used SnCl_2 as a reducing agent of the $[\text{}^{188}\text{ReO}_4]^-$ and $[\text{}^{99\text{m}}\text{TcO}_4]^-$ species, directly eluted from the corresponding generators [12]. The strongly acid medium is required to prevent the formation of undesired SnCl_2 hydrolysis subproducts, as well as to provide chloride ions as anionic ligands.

The reaction of KReO_4 and PTA in the presence of SnCl_2 occurred under mild conditions, stirring the solution at 40°C . After 30 minutes, a solid product started to precipitate and the complete separation was obtained by evaporation of the solvent.

On the basis of details given below, we tentatively formulated the dark orange crystalline product, recovered in good yield (85% based on KReO_4), as the cationic Re(IV) complex $[\text{ReCl}_3(\text{PTA})_3]\text{Cl}$ (**1**), (Scheme 1).



Scheme 1

The $^{31}\text{P}\{^1\text{H}\}$ NMR spectrum of **1** recorded in D_2O presents no signal, suggesting the paramagnetic nature of the species in solution. In contrast, ^1H NMR spectrum showed a sequence of singlets and doublets between 6.78 and 13.20 ppm, due to the P- CH_2 -N (singlet) and N- CH_2 -N (doublet, $^2J_{\text{HH}} = 12.9 \text{ Hz}$) protons of the coordinated phosphaadamantane cage [29].

Although these ^1H chemical shift values appear unusual compared with the corresponding signals of PTA in diamagnetic species [14], peaks assignment is possible on the basis of the characteristic multiplicity and of the integrals values. Two species in a 1:1 ratio can be constantly recognised in various batches from different preparations. We identified them as two *fac* and *mer* isomers, which is plausible for a rhenium complex containing three PTA in an octahedral geometry, and considering also that the cone angle of PTA (103°) is narrow in comparison with that of other alkyl- and aryl-phosphines. Monitoring the solution of **1** in D_2O over two weeks, the appearance of the signals and the isomeric ratio were found unchanged.

Regarding the exact composition of complex **1**, because of the acidity of the reaction medium, we cannot exclude the presence of PTA in its *N*-protonated form, $(\text{PTA-H})^+$, which, in spite of the likely reduction of nucleophilicity, is still able to coordinate through electrons donation from phosphorous [7,8]. The fast proton scrambling among the three nitrogen atoms of $(\text{PTA-H})^+$ prevents the loss of symmetry and justifies the observation of a single signal for P- CH_2 -N and a single signal for N- CH_2 -N, for each isomer [29].

Moreover, the ESI-MS isotopic pattern of the $[\text{ReCl}_3(\text{PTA})_3]^+$ fragment, observed at 764 m/z (80%), is in perfect agreement with the calculated (764.03), supporting the composition of **1**.

The IR spectrum showed the characteristic broad bands of water (3521, 2983, 1666 cm^{-1}), in addition to the bands related to the phosphaadamantane cage (1450 – 580 cm^{-1} , see *Experimental section*).

We found a variability in the elemental analysis of different samples of **1**, which could be related to a variable amount of water content. Attempts to completely eliminate water by heating in vacuum or drying on P₂O₅, caused partial decomposition of the product.

Complex **1** is very soluble in water (S_{20 °C} (H₂O): 0,8 g mL⁻¹) and less soluble in common polar solvents (MeOH, EtOH, acetone). It is stable either in solution or in solid state, also in the presence of oxygen and of light.

Under the above reported reacting conditions, the metal reduction led to Re(IV) complex **1**, but the formation of the pursued *oxo*-derivatives of Re(V) was not observed.

By considering that in the presence of SnCl₂ reduction of Re(VII) reached Re(IV), we tried to repeat the reaction excluding SnCl₂ (Scheme 1). The acidic aqueous mixture of KReO₄ and PTA was heated at 40°C and, in about 40 minutes, a colour change from yellow to brown-orange was observed together with the separation of microcrystals, which were isolated and characterized both in solution and in the solid state.

The ¹H NMR spectrum of complex **2** in D₂O showed two sets of signals in a 1:4 ratio between 11.8 and 5.0 ppm, which are indicative of paramagnetic and isomeric species. The methylene protons of the PTA cage showed signals with a shape comparable to that found in complex **1**, but two new additional singlets, each integrating three protons each, were surprisingly observed at 5.04 and 5.19 ppm, for the major and minor species respectively.

In the MS-ESI spectrum of **2**, the isotopic pattern observed for [M]⁺ at 672 m/z (54%), was surprisingly consistent with the molecular formula [ReCl₄(PTA-Me)₂]⁺.

Crystals suitable for diffractometric analysis were obtained and the product was unequivocally identified as a tetra-chloride complex of Re(III) with two *N*-methylated PTA in *cis* disposition, [ReCl₄(PTA-Me)₂]Cl, **2** (Scheme 1). An ORTEP view of **2** is reported in Figure 1 while selected bond lengths and angles are listed in Table 2.

The structurally characterized complex **2** is probably the less soluble of the two species observed in solution by ¹H NMR, it is reasonably a *cis/trans* couple of isomers also in this case too.

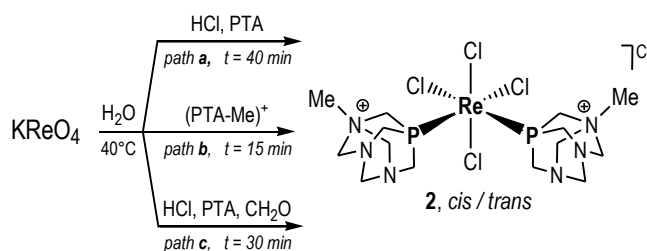
With the aim of gathering information to support this hypothesis, the fully optimized geometry of the *cis*-[ReCl₄(PTA-Me)₂]⁺ and *trans*-[ReCl₄(PTA-Me)₂]⁺ cations were obtained in water by density functional theory (DFT) calculations carried out at the B3LYP/LanL2DZ level of theory. The energies of the two isomers were found to be very close to each other, the *cis* molecule being more stable than the *trans* one by only 2.7 kcal/mol. This result seems to be a clear indication of the coexistence of the two isomers in solution, with a possible prevalence of the *cis* form.

While the X ray crystal structure of **2** allowed a undeniable identification of the complex, the origin of the presence of two (PTA-Me)⁺ ligands, instead of the expected PTA, still needed to be

explained. The *N*-alkylation of PTA takes generally place by treatment of PTA with the appropriate alkyl halide, as we and other reported before [13,14, 15-18] but D.J. Daigle *et al* noticed that both PTA and PTA(O), gave the corresponding methylated forms when treated with formaldehyde in the presence of hydrochloric acid [30].

In order to clarify the mechanism of the unexpected transformation, we repeated the reaction several times, collecting the following observations: *i*) the yields were always low (ca.50%); *ii*) the characteristic formaldehyde smell was perceived, developing from the reaction; *iii*) larger was the amount of hydrochloric acid in the initial mixture, faster was the reaction and the formaldehyde development. These observations are consistent with a redox process, favored by the acid medium, where the oxidation of PTA by KReO_4 occurs simultaneously to its partial decomposition with formaldehyde release.

As a comparison experiment, we prepared an acid solution of KReO_4 with an excess of PTA and then we added a solution of CH_2O . Complex **2** was promptly obtained in good yield (Scheme 2, *path c*). Another confirmation experiment was carried out replacing PTA with pre-formed (PTA-Me)⁺: the formation of **2** was completed in 15 minutes with high yield, (Scheme 2, *path b*). Therefore, we can ascribe the low yield of our reaction (Scheme 2, *path a*) to a partial decomposition of the PTA ligand, which acts as a source of CH_2O , responsible of the methylation of PTA. The high speed of the process did not allow us to understand if the PTA methylation occurred before or after the coordination.



Scheme 2

The reaction of KReO_4 and PTA in D_2O with an excess of HCl was also monitored by multinuclear NMR spectroscopy using a 5-mm screw-cap NMR tube. The singlet at -90.88 ppm in the $^{31}\text{P}\{^1\text{H}\}$ NMR spectrum was consistent with the instantaneous formation of $[\text{PTA}(\text{H})]^+$. When the yellow solution was heated at 40°C in an oil bath for 10 minutes, the development of small bubbles was noticed and a singlet at 9.9 ppm, attributable to the free formaldehyde, was observed in the protonic spectrum. The signal of $[\text{PTA}(\text{O})]$ at -3.14 ppm then appeared in the corresponding $^{31}\text{P}\{^1\text{H}\}$ NMR spectrum. The presence of formaldehyde in the warm and acidic environment,

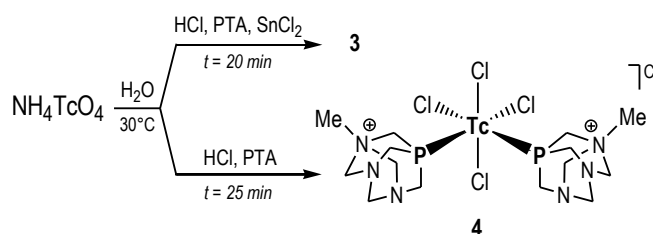
favours the formation of $[\text{PTA}(\text{Me})]^+$ both in the free forms, as showed by $^{31}\text{P}\{^1\text{H}\}$ NMR (-85.50 ppm), and in the coordinated form, as found in complex **2**. As previously reported, when the reaction was made on a large scale, the stability of complex **2** and its tendency to crystallize, allowed to separate the product from the reaction solution with a good purity.

3.2. Technetium complexes **3** and **4**

In order to obtain analogue water-soluble Tc complexes, hopefully exploitable as precursors for radiopharmaceuticals, we tried to reproduce with Tc the above described reactivity, observed for Re. To a water solution containing $\text{NH}_4[\text{TcO}_4]$, an excess of HCl, SnCl_2 and PTA were added in sequence. The mixture, stirred and heated at 30°C , was then left at room temperature until red microcrystals separated. The presence of paramagnetic species did not allow us to identify the product by NMR and several attempts to obtain crystals suitable for an X-ray analysis were unsuccessful. This reaction, repeated several times, gave the same product, i.e., red microcrystals that we tentatively formulated as $[\text{TcCl}_3(\text{PTA})_3]\text{Cl}$, (**3**) for analogy with the corresponding Re product, (Scheme 3).

When the reaction was repeated without SnCl_2 , the colorless solution turned to a persistent deep orange coloration, indicating the end of the reaction, and red crystals slowly separated in about 25 minutes. The ^1H -NMR spectrum showed broad signals in the range from 7.4 to 13.4 ppm, characteristic of a paramagnetic species. In the $^{31}\text{P}\{^1\text{H}\}$ NMR spectrum, signals were not observed due to the quadrupole effect of the metal core [31, 32].

We managed to produce crystals suitable for diffractometric investigation: the X-ray analysis showed a structure similar to that observed for complex **2**, with two $(\text{PTA}-\text{Me})^+$ coordinated to the metal center to give $[\text{TcCl}_4(\text{PTA}-\text{Me})_2]\text{Cl}$, (**4**), (Scheme 3). An ORTEP view is shown in Figure 2 and selected bond lengths and angles are given in Table 2.

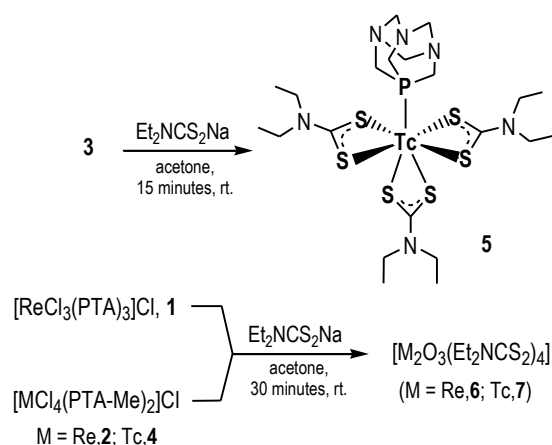


Scheme 3

3.3. Reactions of PTA complexes **1-4** with $\text{Na}(\text{Et}_2\text{NCS}_2)$

With regard to the reactivity of the above discussed complexes **1-4**, we tested the possibility of replacing two monodentate ligands with a bidentate dithiocarbamate; the aim was to obtain new Re and Tc complexes associating hydrophilic PTA with the chelating monoanionic ligand $(\text{RNCS}_2)^-$ ($\text{R} = \text{Et}$). The coordination of dithiocarbamate on Re and Tc has been widely studied and several products have been prepared and fully characterized. In fact, the $\text{M}-\text{S}_2\text{CNR}_2$ fragment ($\text{M} = \text{Re}, \text{Tc}$) can introduce a variety of organic functionalities R that are useful for the development of new radiopharmaceutical compounds; at this regard the well-known compound TcN-NOET [bis(N-ethoxy,N-ethylthiocarbamato) nitrido-Tc(V), $[\text{}^{99\text{m}}\text{Tc}(\text{N})(\text{NOEt})_2]$], has been proposed as a myocardial imaging agent [33- 35].

The reaction of the tentatively identified complex **3** with a small excess of $(\text{Et}_2\text{NCS}_2)^-$, under gentle heating for 15 minutes, produced yellow-brown microcrystals after evaporation of the solvent, (Scheme 4). The ^1H NMR of the diamagnetic product showed the signals of the PTA cage as well as those of the protons of the ethyl moiety of the $(\text{Et}_2\text{NCS}_2)^-$ ligands. The X-ray structure, reported in Figure 3, unequivocally identified it as complex $[\text{Tc}(\text{Et}_2\text{NCS}_2)_3(\text{PTA})]$ (**5**), containing an unusual epta-coordinated technetium (III) with three diethyldithiocarbamate and one PTA ligand in apical position, in a distorted pentagonal-bipyramidal geometry. This arrangement is similar to that reported by Baldas for the carbon monoxide complex $[\text{Tc}(\text{Et}_2\text{NCS}_2)_3(\text{CO})]$, [30].



Scheme 4

We also tested the reactivity of complexes **1**, **2** and **4** with the diethyldithiocarbamate ligand, using a similar procedure. Each metal complex was treated in solution with a small excess (2.5 equivalents) of $\text{Na}(\text{Et}_2\text{NCS}_2)$; the reaction mixtures were kept at room temperature for 15-30 minutes under stirring and crystalline products (**6** for Re and **7** for Tc) were obtained in good

yields (80-85%, Scheme 4). No difference was observed on heating the mixtures or changing the stoichiometric ratio of the reagents.

The characterization of both **6** and **7** was consistent with the diamagnetic binuclear μ -*oxo* species $[M_2O_3(Et_2NCS_2)_4]$ (M = Re, Tc), revealing that all the PTA ligands were been displaced.

Both **6** and **7** were identified by diffractometric analysis: complex **6** is known and has been reported [22] while complex **7**, $[Tc_2O_3(Et_2NCS_2)_4]$, has not been characterized before.

An ORTEP view of **7** is shown in Figure 4, while the selected bond distances and angles are listed in Table 2.

3.4. Structures description

ORTEPIII [31] diagrams for complexes **2**, **4**, **5** and **7** are shown in Figures 1 - 4 respectively. Complexes **2** and **4** show a very similar geometry. In both structures the metal atoms are linked to four chlorine and two Me-PTA ligands to give a slightly distorted octahedral geometry, the P1-Re/Tc-P2 angle values significantly deviating from the ideal value of 90° because of the steric hindrance of the two PTA ligands in *cis* position (Table 2). Besides the Cl⁻ counterion, the asymmetric unit of both complexes is completed by co-crystallized water molecules; in **2**, however, they have been found to be highly disordered and were not included in the refinement (*vide supra*).

The neutral Tc(V) complex **7** is dinuclear, with O=Tc-O-Tc=O backbone. The distorted octahedral coordination of each Tc atom is completed by two bidentate diethyldithiocarbamate ligands.

The Tc=O and Tc-O distances do not show any significant discrepancy from structural parameters of related Tc(V) complexes. Conversely, in **5** the technetium atom is seven-coordinated and displays a distorted pentagonal-bipyramidal geometry, being linked to three diethyldithiocarbamate and one PTA ligands; the apical positions are occupied by P1 and S5 atoms (P1-Tc-S5= $171.63(3)^\circ$, Table 2). In both **5** and **7** complexes, Tc-S distances are in close agreement with the bond lengths found in other Tc complexes with similar ligands (CSD search, 26 hits) for which a mean value of $2.46(4) \text{ \AA}$ has been calculated. In this respect, is worth comparing the geometry of **5** with that of the very similar complex $[Tc(Et_2NCS_2)_3(CO)]$ where a CO molecule is in place of PTA [40].

The coordination geometry of this complex is pentagonal-bipyramidal, with apical positions occupied by the CO ligand and one S atom (C-Tc-S5= 173.2°). The Tc-S bond lengths, in the range 2.476 - 2.520 \AA , are strictly comparable with those listed in Table 2; in particular, the longest distance involves the apical S atom, as observed in **5**. These findings seem to indicate that the

geometry around the central atom is established by the chelate ligands, irrespective of the nature of the third bound molecule.

In **2** and **4**, besides electrostatic forces of attraction, the different units interact with each other mainly through weak C–H...O and C–H...Cl intermolecular interactions, listed in Table 3 in the Supplementary Materials. The cocrystallized water molecules certainly play a role in lattice stabilization by forming stronger hydrogen bonds, as shown by the very short Ow...Ow distance found in **4** (2.756(8) Å).

Comparable weak C–H...O/S interactions are found in the crystal structure of **7**. In **5**, no interatomic contact shorter than the sum of the van der Waals radii was found. The packing patterns are reported in Figure 5 for complexes **2**, **4**, **5** and **7**, respectively.

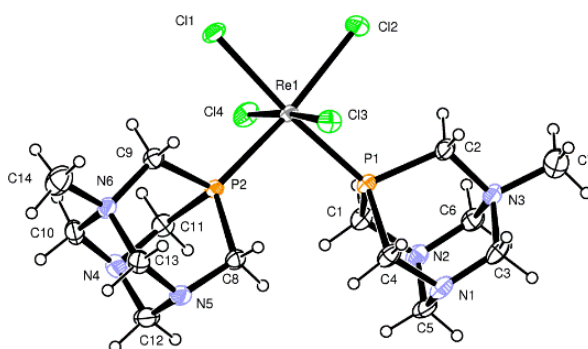


Figure 1. ORTEPIII view and atom numbering scheme for complex **2**. Thermal ellipsoids are drawn at the 40% probability level. The Cl⁻ counterion is not shown.

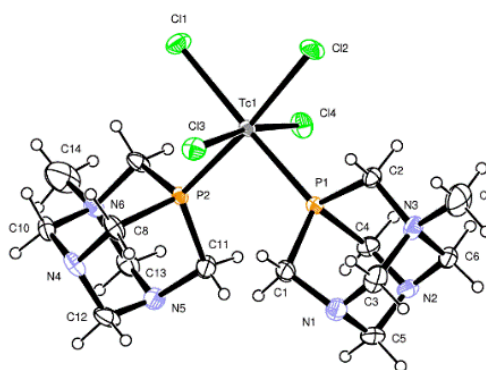


Figure 2. ORTEPIII view and atom numbering scheme for complex **4**. Thermal ellipsoids are drawn at the 40% probability level. The Cl⁻ counterion and the solvent molecules are not shown.

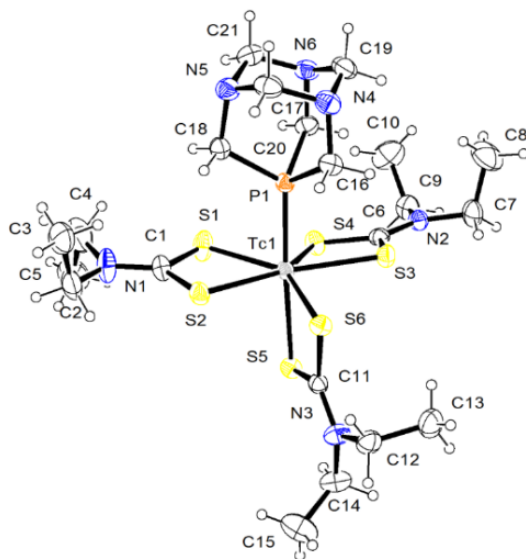


Figure 3. ORTEPIII view and atom numbering scheme for complex **5**. Thermal ellipsoids are drawn at the 40% probability level.

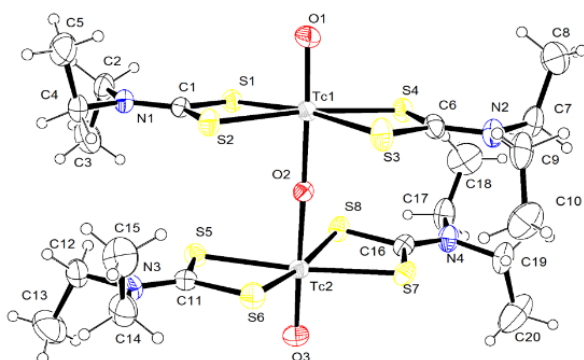


Figure 4. ORTEPIII view and atom numbering scheme for complex **7**. Thermal ellipsoids are drawn at the 40% probability level.

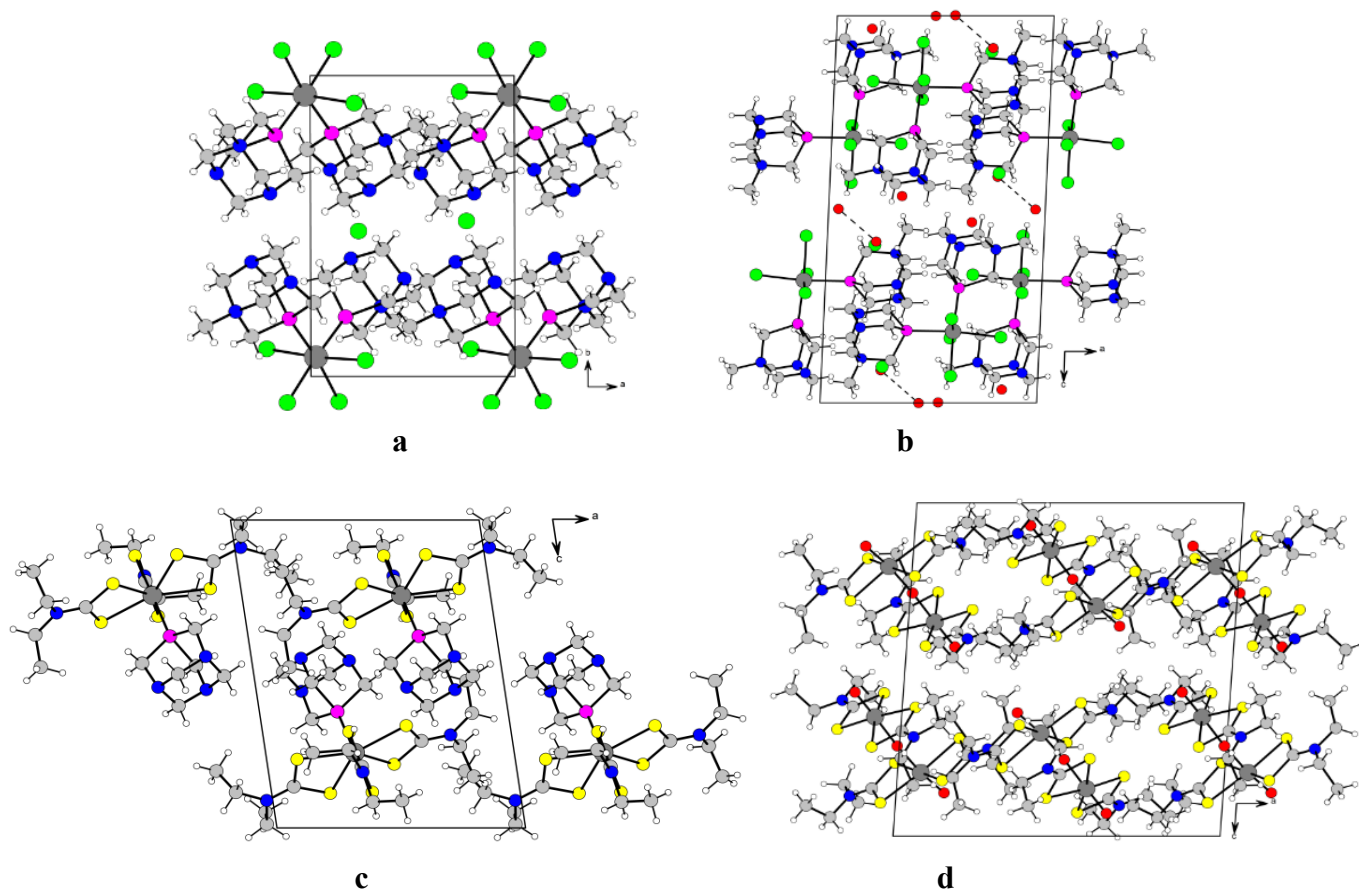


Figure 5. Unit cell content of complex **2**, (**a**) (viewed down *c*). O...O short contacts are shown as dashed lines; complex **4**, (**b**), (viewed down *b*); complex **5**, (**c**), (viewed down *b*); complex **7**, (**d**), (viewed down *b*).

4. Conclusions

The paramagnetic water soluble complexes **1-4** containing the hydrophilic phosphines PTA or (PTA-Me)⁺ were obtained directly from the tetra-oxo-permetallated anions [ReO₄]⁻ and [TcO₄]⁻, isotopomers of [¹⁸⁸ReO₄]⁻ and [^{99m}TcO₄]⁻, the species eluted from the respective generators, used in nuclear medicine.

The Re(IV) and Tc(IV) complexes **1** and **3**, produced by reaction of [ReO₄]⁻ and [TcO₄]⁻ with PTA and SnCl₂, were soluble in water and stable in solution as well as in the solid state.

When SnCl₂ was excluded, the unexpected species containing M(III) and methylated PTA [MCl₄(PTA-Me)₂]Cl, (M = Re, **2**; Tc, **4**) were isolated, due to the partial decomposition of PTA in the acid medium, occurring with release of formaldehyde, which gave the corresponding (PTA-Me)⁺.

The reactions of the new complexes **1**, **2** and **4** with diethylthiocarbamate occurred with total displacement of PTA and produced the diamagnetic binuclear μ -oxo species [M₂O₃(Et₂NCS₂)₄] (M = Re, **6**; Tc, **7**). The reaction of **3** gave instead complex **5**, [Tc(Et₂NCS₂)₃(PTA)], which shows an unusual epta-coordinated technetium(III), with three bidentate diethyldithiocarbamate and one PTA in apical position. Because of their favourable characteristics like the simplicity in preparation from aqueous solution of permetallated salts, the solubility and stability in water, the new complexes **1**, **2**, **4**, and **5** deserve to be further studied and developed for pharmaceutical applications.

Acknowledgments

We thank Dr T. Bernardi, Dr E. Bianchini and Dr P. Formaglio for technical assistance, Dr. R. Amadelli and CIRCMSB (Consorzio Interuniversitario di Ricerca in Chimica dei Metalli nei Sistemi Biologici) for support.

References

- [1] G. R. Morais, A. Paulo, I. Santos, *Organometallics* 31 (2012) 5693–5714.
- [2] G. De Tommaso, V. Celentano, G. Malgieri, R. Fattorusso, A. Romanelli, L. D. D'Andrea, M. Iuliano, C. Isernia, *Chemistry Select* 1 (2016) 3739-3744.
- [3] T. Ganguly, B.B. Kasten, T.R. Hayes, P. D. Benny, *Advances in Chemistry Research, Review* 18 (2013) 93-141.
- [4] B. Goins, W. T. Phillips, A. Bao, *Methods in Molecular Biology* (Clifton, N.J.) 1522 (2017) 155-178.

- [5] N. Pfannkuchen, M. Meckel, F. Rosch, R. Bergmann, M. Bachmann, C. Bal, M. Sathekge, W. Mohnike, R.P. Baum, *Pharmaceuticals*, Review 10 (2017) 2.
- [6] L. Kenneth Kam-Wing, *Acc. Chem. Res.* 48 (2015) 2985-2995.
- [7] B. Goins, A. Bao, W.T. Phillips, *Methods in Molecular Biology* (Clifton, N.J.) 606 (2010) 469-91.
- [8] J. Lecina, O. Palacios, S. Atrian, M. Capdevila, J. Suades, *JBIC* 20 (2015) 465-474.
- [9] A. Leonidova, G. Gasser, *Chemical Biology*, 9 (2014) 2180-2193.
- [10] A. Boschi, A. Duatti, L. Uccelli, *Topics in Current Chemistry*, Review 252 (2005) 85-115.
- [11] P.V. Grundler, L. Helm, R. Alberto, A.E. Merbach, *Inorg. Chem.* 45 (2006) 10378-10390.
- [12] W. Xiangyun, W. Yonghui, W. Y., L. Yuanfang, *J.N.R.S.* 1 (2000) 15-18.
- [13] J. Bravo, S. Bolaño, L. Gonsalvi, M. Peruzzini, *Coord. Chem. Rev.* 254 (2010) 555-607.
- [14] A D. Phillips, L. Gonsalvi, A. Romerosa, F. Vizza, M. Peruzzini, *Coord. Chem. Rev.* 248 248 (2004) 955-993.
- [15] P. Bergamini, L. Marvelli, A. Marchi, F. Vassanelli, M. Fogagnolo, P. Formaglio, T. Bernardi, R. Gavioli, F. Sforza, *Inorg. Chim. Acta* 391 (2012) 162-170.
- [16] D.A. Krogstad, K. E. Gohmann, T.L. Sunderland, A. L. Geis, P. Bergamini, L. Marvelli, V. G. Young Jr., *Inorg. Chim. Acta* 362 (2009) 3049.
- [17] P. Bergamini, L. Marvelli, A. Marchi, V. Bertolasi, M. Fogagnolo, P. Formaglio, F. Sforza, *Inorg. Chim. Acta* 398 (2013) 11-18.
- [18] V. Ferretti, M. Fogagnolo, A. Marchi, L. Marvelli, F. Sforza, P. Bergamini, *Inorg. Chem.* 53 (2014) 4881-4890.
- [19] A. Marchi, E. Marchesi, L. Marvelli, P. Bergamini, V. Bertolasi, V. Ferretti, *Eur. J. Inorg. Chem.* (2008) 2670-2679.
- [20] D. Daigle, A. Pepperman, S. L. Vail, *J. Heterocyclic Chem.* 11 (1974) 407-408.
- [21] D.J. Daigle, A.B. Pepperman Jr., *J. Heterocyclic Chem.* 12 (1975) 579-580.
- [22] S. R. Fletcher, J. F. Rowbottom, A. C. Skapski and G. Wilkinson, *J. Chem. Soc. D* (1970) 1572b-1573.
- [23] C. W. Carter, R. M. Sweet Eds.; Academic Press London, Vol. 276, Part A (1977) 307-326.
- [24] R. H. Blessing, *Acta Crystallogr.* A51 (1995) 33-38.
- [25] Altomare, M.C. Burla, M. Camalli, G. Cascarano, C. Giacovazzo, A. Guagliardi, A.G. Moliterni, G. Polidori and R. Spagna, *J. Appl. Crystallogr.* 32 (1999) 115-119.
- [26] G. M. Sheldrick, *Acta Crystallogr.* A64 (2008) 112-122.
- [27] L. J. Farrugia, *J. Appl. Crystallogr.* 32 (1999) 837-838.
- [28] L. Spek, *J. Appl. Crystallogr.* 36 (2003) 7-13.
- [29] P. Smoleński, A. J. L. Pombeiro, *Dalton Trans.* (2008) 87-91.
- [30] D.J. Daigle, A.B., Pepperman, S.L. Vail, *J. Heterocyclic Chem.* 11 (1974) 407-408.
- [31] L. A. O'Connell, R. M. Pearlstein, A. Davison, J. R. Thornback, J. F. Kronauge and A. G. Jones, *Inorg. Chim. Acta* 161 (1989) 39-43.
- [32] U. Abram, B. J. Lorenz, L. Kaden and D. Scheller, *Polyhedron* 7 (1988) 285-289.
- [33] N. Salvarese, N. Morellato, A. Rosato, L. Melendez-Alafort, F. Refosco, C. Bolzati, *J. Med. Chem.* 57 (2014) 8960-70.
- [34] N. Salvarese, N. Morellato, A. Venzo, F. Refosco, A. Dolmella, C. Bolzati, *Inorg. Chem.* 52 (2013) 6365-6377.
- [35] C. Bolzati, M. Cavazza-Ceccato, S. Agostini, F. Tisato, G. Bandoli, *Inorg. Chem.* 47 (2008) 11972-11983.

- [36] R. Pasqualini, A. Duatti, *J. Chem. Soc. Chem. Commun.* (1992) 1354-1355.
- [37] R. Pasqualini, A. Duatti, E. Bellande, V. Comazzi, V. Brucato, D. Hoffschir, D. Fagret, M. Comet, *J. Nucl. Med.* 35 (1994) 334-341.
- [38] F. Tisato, C. Bolzati, F. Refosco, M. Porchia, R. Seraglia, D. Carta, R. Pasqualini, *Nucl. Med. Biol.* 39 (2012) 335-346.
- [39] J. Baldas, J. Bonnyman, P. M. Pojer, G. A. Williams, M. F. Mackay, *J. Chem. Soc., Dalton Trans.* (1982) 451-455.
- [40] M.N. Burnett, C.K. Johnson, ORTEP III. Report ORNL-6895, Oak Ridge National Laboratory, Oak Ridge, Tennessee, USA, 1996.